Journal of Advanced Scientific Research

Available online through https://sciensage.info

ISSN
0976-9595
Research Article

GREEN SYNTHESIS OF CHROMIUM OXIDE NANOPARTICLES - STUDY OF ITS ANTIBACTERIAL, PHOTOCATALYTIC AND THERMODYNAMIC PROPERTIES

Duraivathi C.*[1, e], Jeya Priya J.[2, e], Poongodi J.[3, e], Johnson JeyakumarH.[4, e]

[1]*Department of physics (Reg. no. 18212152132004), Pope's College, Sawyerpuram,Tamil Nadu, India*
[2]*Department of physics V. O. Chidambaram College, Thoothukudi, Tamil Nadu, India*
[3]*Department of physics, Kamaraj College, Thoothukudi, Tamil Nadu, India*
[4]*Department of physics (Reg. no. 19112232132024), Pope's College, Sawyerpuram,Tamil Nadu, India*
[e]*Affiliated to Manonmanium Sundaranar University, Abishekapatti, Tirunelveli, Tamil Nadu, India*
**Corresponding author: cduraivathikamali@gmail.com*

Received: 23-08-2022; Accepted: 07-10-2022; Published: 31-10-2022

 https://doi.org/10.55218/JASR.202213904

ABSTRACT

An endeavor has been made to report the herbal synthesis of chromium oxide (Cr_2O_3) nanoparticles using aqueous extract of *nigella sativa* seed extract as a capping agent and chromic sulphateas a precursor material. The structural, morphological and optical properties of the Cr_2O_3 nanoparticles were analyzed by X - ray diffraction (XRD), Fourier transform infrared spectroscopy (FTIR), Scanning electron microscopy (SEM) and UV- Visible spectroscopy. The antibacterial efficacy of chromium oxide nanoparticles was tested against *Staphylococcus aureus*, *Klebsiella pneumonia* and *Pseudomonas aeruginosa*. The photocatalytic activity of biosynthesized Cr_2O_3 nanoparticles was evaluated by degrading methylene blue dye and Congo red dye under the irradiation of visible light. Apart from this, ultrasonic velocity, density and viscosity were measured for different concentrations of Cr_2O_3 nanofluid using ultrasonic techniques. Thermoacoustical such as adiabatic compressibility, free length, acoustic impedance, relaxation time and absorption coefficient values are computed from the measured data and the results are interpreted in terms of particle - fluid interactions.

Keywords: Capping agent, Antibacterial, Photocatalytic, Irradiation, Velocity, Absorption coefficient.

1. INTRODUCTION

Green nanotechnology, which employs biosynthetic techniques and environment friendly approaches to synthesis nanoparticles, is one of the most important and rapidly evolving areas in scientific research. The creation of nanoscale metal and metal oxides, such as cadmium oxide [1], cobalt oxide [2], zirconium oxide [3], calcium oxide etc., are of considerable interest owing to their enhanced thermal conductivity, good catalytic activity, remarkable antimicrobial activity, easy availability of economical and up-scaled synthetic approaches and low toxicity. Among various metal oxides-based nano-particles, Cr_2O_3 nanoparticle, is of high significance and interest because of its unique physicochemical properties such as a wide band gap (~3.4 eV), high melting temperature, and increased stability [4] and also Cr_2O_3 is the most stable magnetic-dielectric oxide-material [5]. The Cr_2O_3 nanoparticles have been widely utilized in different applications, including catalysis, photonics, coating materials, advanced colorants, etc. [6-8]. Various methods have been reported for the preparation for chromium nanoparticles such as hydrothermal [9, 10], sol-gel [11], combustion [12], precipitation [13], gelatin [14], microwave irradiation [15] micro-emulsion [16] method.

Among all these methods mentioned above, an attempt has been made to report the synthesis of Cr_2O_3 nanoparticles through sol - gel method by using *Nigella sativa* seed extract as a capping or reduction agent and chromic sulphate ($Cr_2S_3O_{12}$) as a precursor material. The obtained green synthesized Cr_2O_3nanoparticles were elucidated through X-ray diffraction spectroscopy, FT-IR spectroscopy, UV - Visible spectroscopy and scanning electron microscopy.

2. MATERIAL AND METHODS

2.1. Material

Chromic sulphate ($Cr_2S_3O_{12}$) powder was purchased from Avantor Performance Materials India Limited and seeds of *Nigella sativa* were procured from a local market and brought to the laboratory.

2.2. Herbal Synthesis Chromium oxide nano-particles:

One mM of chromic sulphate ($Cr_2S_3O_{12}$) powder was thoroughly dissolved in 100 ml of nigella sativa seed extract. The color of the reactant solution turned to yellowish brown to dark green. The prepared solution was stirred with a magnetic stirrer for 20 hour and left overnight without any disturbance. The precipitate was washed with ethanol and distilled water after the upper solution was discharged. The dark green precipitate was then dried at 180°C in a hot air oven before being calcined in a muffle furnace at 500°C, 600°C and 700°C for 120 minutes. Finally green colored chromium oxide nanoparticles were obtained.

3. RESULTS AND DISSCUSSION

3.1. XRD Analysis

The crystallinity of the synthesized Cr_2O_3 nanoparticles is analyzed by X- ray diffraction spectroscopy and the results are depicted in fig. 1. The Calcination is a one of the common methods that used to give the improve structure of Cr_2O_3 [17]. The structure of the chromium oxide nanopowders (Cr_2O_3) were characterized at 500°C, 600°C and 700°C for 120 minutes and the results are depicted in fig. 1. At 500°C no peaks were observed and some small peaks were exhibited at 600°C whereas XRD pattern at 700°C elucidates the sharp and intense peaks which parallel to the chromium oxide observed at various angular positions (2Θ) are 24.64°, 33.83°, 36.37°, 40.01°, 41.65°, 44.41°, 50.38°, 55.01°, 57.55°, 58.46°, 63.69°, 65.26°, 67.73°, 71.32°, 73.16°, 77.10°, 79.21°, 84.37° and 86.74° which are indexed to the planes (012), (104), (110), (006), (113), (202), (024), (116), (211), (122), (214), (300), (208), (1010), (217), (306), (0210) and (0012) respectively.

These peak values match well with the JCPDS file no.#840314 and this confirm the rhombohedral structure of green synthesized Cr_2O_3 nanoparticles calcined at 700°C. The lattice constant of Cr_2O_3 nanostructure is found to be a = b = 4.923 Å and c= 13.495 Å.

3.2. DLS spectral Analysis

The dynamic light scattering analysis of Cr_2O_3 nano-particles is depicted in fig. 2. The size of the fabricated chromium oxide nano particles is determined from dynamic light scattering (DLS) study. DLS study revealed that the average particle size of chromium oxide nanoparticles is 87.86 nm. Size determined using DLS is in hydrodynamic size, usually the size determined are large as compared with that from TEM [18].

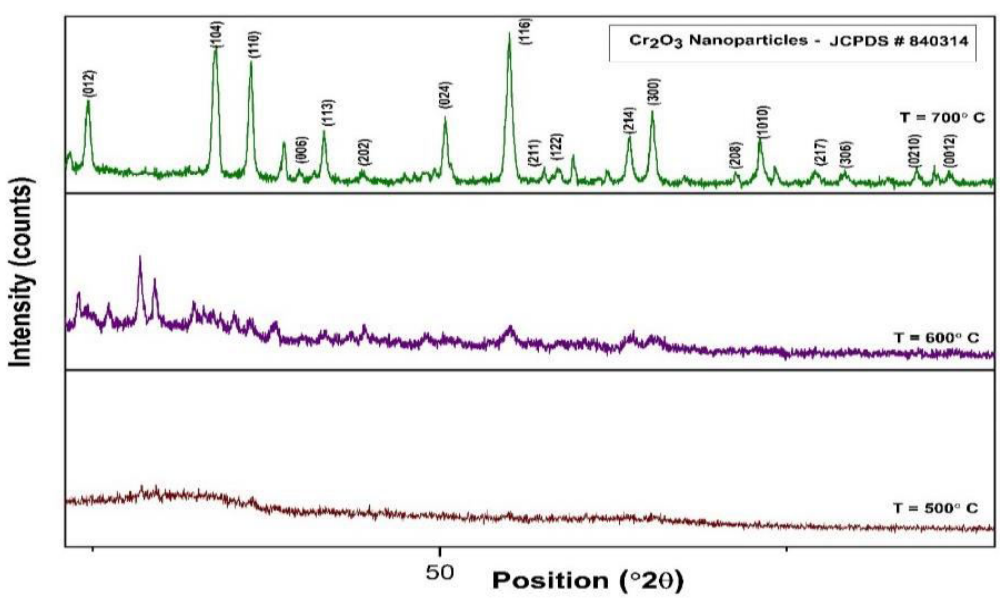

Fig. 1: X – ray diffraction pattern of synthesized Cr_2O_3 nanoparticles

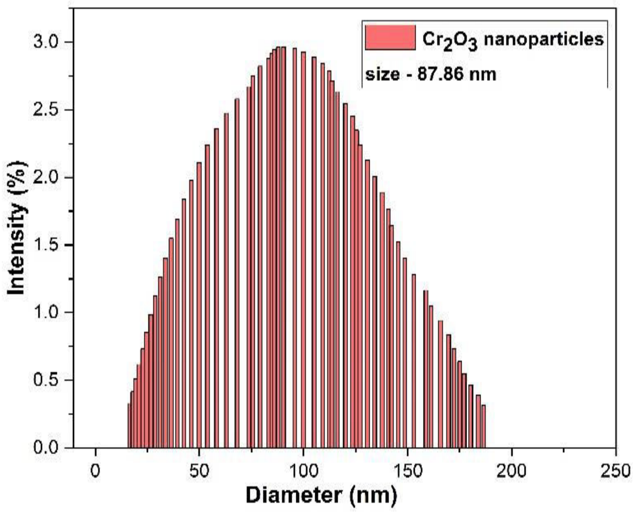

Fig. 2: Dynamic light scattering spectra of Cr_2O_3 nanoparticles

3.3. EDS Spectra Analysis

EDS spectra used to confirm the elemental composition of green synthesized Cr_2O_3 nanoparticles. Fig. 3 illustrates the EDX spectra of the Cr_2O_3 nanoparticles calcined at 700°C temperature. The results clearly explains the presence of the elements Cr and O. Moreover, the atomic percentages of Cr and O are 68.57% and 31.43% respectively.

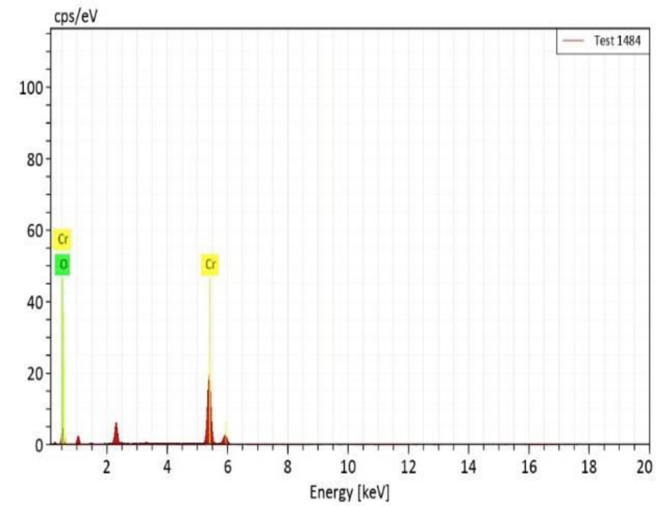

Fig. 3: EDS spectrum of Cr_2O_3 nanoparticles

3.4. Scanning Electron Microscopy Analysis

The surface morphology and shape of synthesized Cr_2O_3 nanoparticles were explored using the scanning electron microscope (SEM) images. The SEM images of green synthesized Cr_2O_3 nanoparticles were shown in fig. 4(a) and 4(b) with the magnification of 1 µm and 200 nmrespectively. The flake morphology of as-grown Cr2O3 nanoparticles can be observed from the figures and the average particle size is found to be 71 nm.

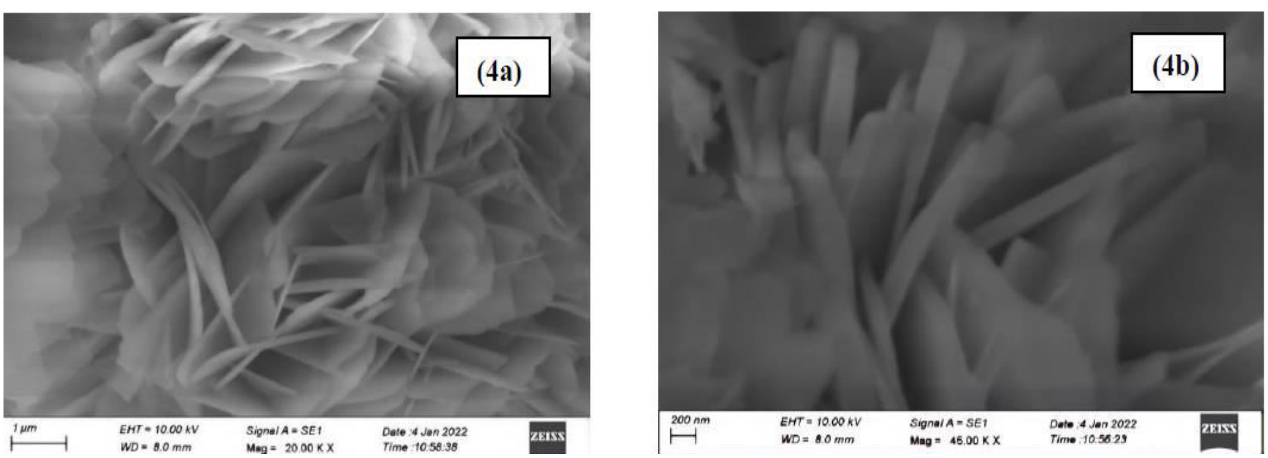

Fig. 4: SEM image of Cr_2O_3 nanoparticles with magnification of (a) 1 µm and (b) 200 nm

3.5. UV - Visible Spectroscopy analysis - Band gap and Optical Transmittance

The absence of absorption in the visible region and maximum transmittance in the whole visible region plays a vital role for NLO applications [19]. The material which possessing high optical transmission employed, inmany applications such as fiber - optic communications, opto - electronic sensors, optical components adhesives and photonics.

The UV-Visible transmission spectrum for the Cr_2O_3 nanoparticles was recorded to know the stability for optical application in the range 100 nm to 1200 nm and it shown in Fig. 5(a). It clearly elucidates that, the synthesized Cr_2O_3 nanoparticles exhibit enhanced transmittance in the entire visible region. The Cr_2O_3 nanoparticles has increased transmittance after 396.707 nm. The optical band gap value was calculated through plot the value $(\alpha h\upsilon)^{1/2}$ versus the value $h\upsilon$ for Cr_2O_3 nanoparticles as illustrated in fig. 5(b). It clearly revealed that, the synthesized Cr_2O_3 nanoparticles has the optical bad gap of 4 eV.

3.6. FT-IR Spectroscopy

FT-IR analysis was performed to characterize the surface chemistry [20] of green synthesized Cr_2O_3 nanoparticles as depicted in fig. 6. The spectrum was recorded for the transmittance band ranging from 4000 cm^{-1} to 500 cm^{-1}. The absorption peak displayed at 3434.63 cm^{-1} represents the hydrogen-bonded O-H groups present in the aqueous phase. The peat at 2922.43 cm^{-1} and 2851.56 cm^{-1} corresponds to the CH_3 stretching vibration. The peak at 2093.57 is attributed to C ≡ C vibration. The presence of N-O asymmetric stretching of nitro compound group is indicated by the peak at 1562.98 cm^{-1}. The absorption peak at 1413 cm^{-1} represents the stretching vibration of -C=O inorganic carbonate group. The peak at 835.29 cm^{-1} is assigned to bending vibration of C=O inorganic carbonate group. The spectra also represent four sharp absorption peaks at 617.71 cm^{-1}, 563.95 cm^{-1}, 443.09 cm^{-1} and 410.57 cm^{-1} which are in well agreement with the reported results [21]. The observed peaks illustrate the characteristic of Cr - O bond stretching vibration. A2u modes are responsible for the bands at 413 cm-1. The structural symmetry in Cr2O3 causes the A2u mode, which is an FTIR vibration mode.

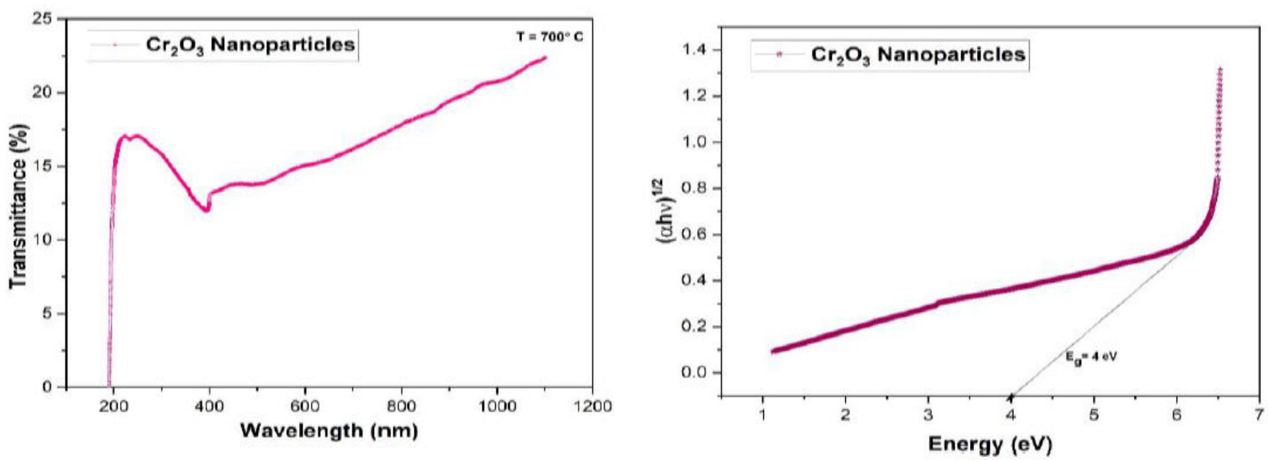

Fig. 5: (a) Transmittance spectra (b) The plots of $(\alpha h\nu)^2$ vs. photon energy of prepared chromium oxide NPs

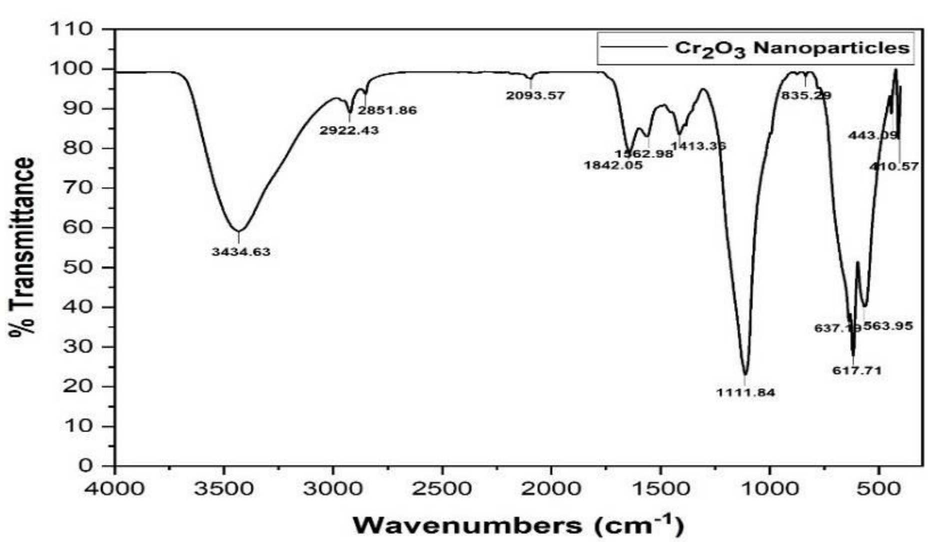

Fig. 6: FTIR spectra of Cr_2O_3 nanoparticles

3.7. Antibacterial activity

The antibacterial effect of green synthesized Cr_2O_3 nanoparticles was evaluated against *Staphylococcus aureus*, *Klebsiella pneumonia* and *Pseudomonas aeruginosa*. The zones of inhibition of Cr_2O_3 NPs against all bacteria are shown in Fig. 7.

The values of zone of inhibition (ZOI) are listed in Table 1. The results demonstrate that, Cr_2O_3 nanoparticles, significantly inhibited against the growth of tested species.

Fig. 7: Antibacterial activity of Cr_2O_3 nanoparticles against *Pseudomonas aeruginosa, Staphylococcus aureus* and *Klebsiella pneumonia* respectively

Table 1: Antibacterial activity data for Chromium Oxide nanoparticles

Bacteria name	Zone of Inhibition (mm) (0.02 mg dose)	Standard value
Staphylococcus aureus	16	20
Klebsiella pneumonia	25	35
Pseudomonas aeruginosa	15	25

3.8. Photocatalytic degradation of synthetic dyes Cr_2O_3 nanoparticles

The photocatalytic activity of Cr_2O_3 nanoparticles was evaluated against the methylene blue dye and congo red dye under the irradiation of visible light. The dye degradation efficacy was tested with various doses of Cr_2O_3 nanoparticles (5 mg, 10 mg) as illustrated in fig.8. Both methylene blue (MB) and congo red (CR) dyes undergoes complete decomposition even at the lower concentration of Cr_2O_3 nanoparticles with the reaction time of 60 minutes. As a result, it was concluded that, Cr_2O_3 nanoparticles hold an enhanced photocatalytic degradation efficacy against both dyes.

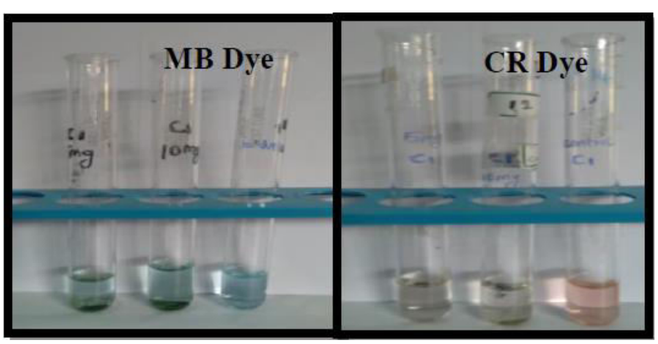

Fig. 8: Dye degradation efficacy of Cr_2O_3 Nps

3.9. Thermoacoustical study of Cr_2O_3 Nanofluids

Nanofluids play a vital role in heat transfer applications. Thermoacoustical and thermodynamical aspects of fluids are all important in understanding the nature of physic-chemical behaviour of liquid and liquid mixtures. An attempt has been made to report the ultrasonic velocity, free length, viscosity and absorption coefficient(α/f^2) for various concentration of Cr_2O_3 nanoparticles (0.01 wt(%), 0.02 wt(%), 0.03 wt(%), 0.04 wt(%) and 0.05 wt(%)) in base fluid at different temperatures as depicted in fig. 9(a), (b), (c),(d).

The non- linear variation of ultrasonic velocity with concentration of Cr_2O_3 nanoparticles as illustrated in fig. 9(a) shows the complex formation and significant particle-fluid interaction. Nevertheless, as temperature increases, ultrasonic velocityin nanofluid decreases which explores strong interaction between particle and fluid molecules in the nanofluid matrix at lower temperature (308 K). The decrease in free length shows decrease in degree of association among the nano-particles and molecules of base fluid depicted in fig. 9(b). From fig. 9(c), it is observed that, viscosity also exhibit the non - linear variation indicates the cohesion among the particle and fluid molecules due to the complex formation. The viscosity attains maximum value at 0.04 wt. % of Cr_2O_3 nanoparticles even at all temperatures depicts the strong molecular association at that concentration. As the concentration of nano-particles increases, the absorption co-efficient decreases, and shows sudden increase in 0.04 wt. % of Cr_2O_3 nanoparticles even at all temperatures as shown in fig.

9(d). The maximum occur at particular concentration may indicate a remote possibility of the formation of an aggregate [22] containing one molecule of Cr_2O_3 nanoparticles and one molecule of base fluid (ethylene glycol) indicates the significant particle-fluid interactions. Hence it concluded that there is a significant interaction present in the Cr_2O_3 nanofluid matrix.

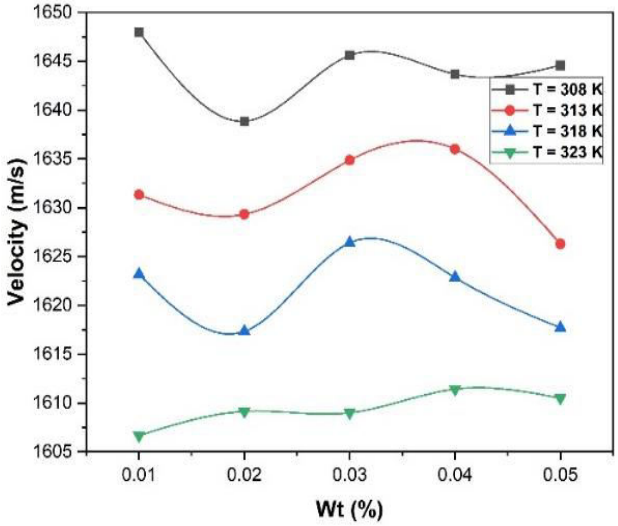

9(a)

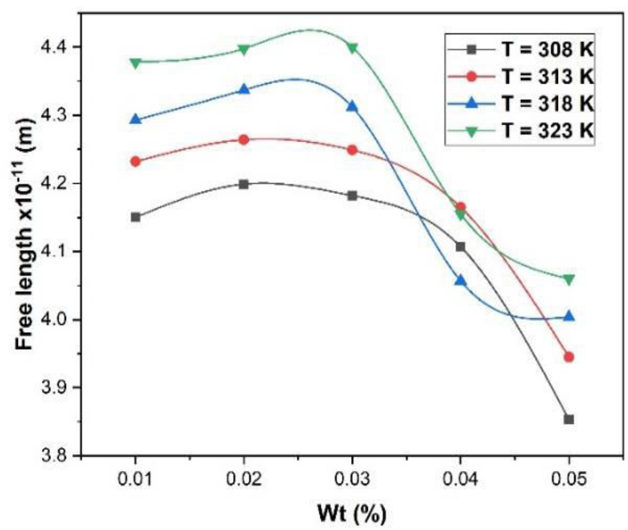

9(b)

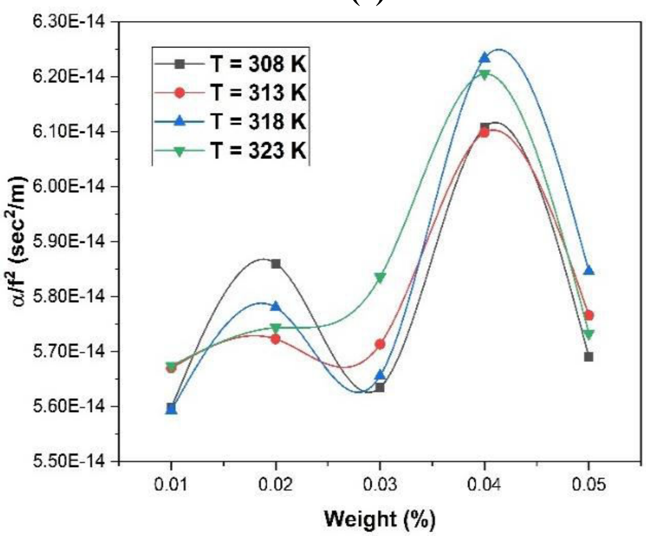

9(c)

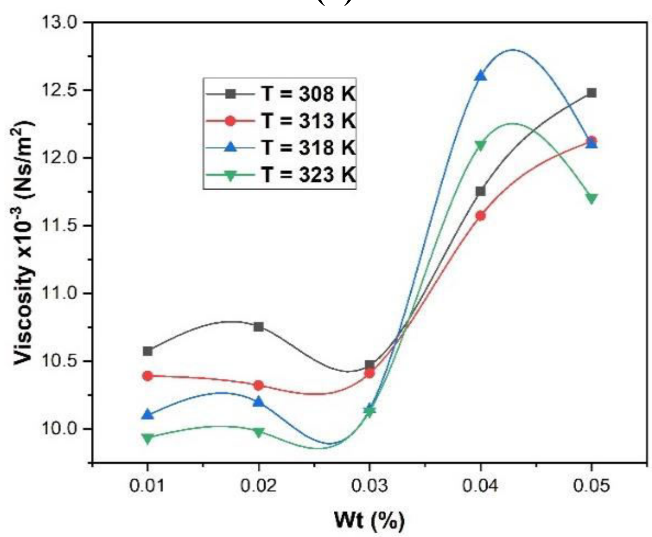

9(d)

Fig. 9: variation of weight (%) with (a) velocity, (b) free length, (c) viscosity, (d) α/f^2.

4. CONCLUSION

The Cr_2O_3 nanoparticles were synthesized using *Nigella sativa* leaf extract as a capping agent through eco-friendly approach. Synthesized nanoparticles were characterized by XRD, EDS, FTIR, UV-Visible spectroscopy and scanning electron microscopy. The average size of the Cr_2O_3 nanoparticles was found to be 71 nm from SEM images and 77 nm from DLS analysis. The band gap of the nanomaterial was found to be 4 eV from the UV-Visible spectroscopy result. The green synthesized Cr_2O_3 nanoparticles show enhanced dye degradation efficacy tested against methylene blue dye, congo red dye and significant antibacterial activity against *Staphylococcus aureus*, *Klebsiella pneumonia* and *Pseudomonas aeruginosa*. Thermoacoustical parameters of Cr_2O_3 nanoparticles in basefluid were studied and it is concluded that there is a significant particle-fluid interactions and it act as a nanofluid for any heat transfer applications.

5. ACKNOWLEDGEMENTS

One of the authors (C. Duraivathi) would like to express her heartfelt thanks to the Director of Collegiate Education, Chennai - 600006 for the stipend provided under the full time Research Scholar Scheme, since 2018.

Conflict of interest

There is no conflict of interest between the authors.

6. REFERENCE

1. Ghotekar S. *Asian J. Green Chem.,* 2019; 3**(2):**187-200.
2. Jeya Priya J, Duraivathi C, Poongodi J, Amudhavalli K. *International Journal of Creative Research thoughts*, 2022; **10**:d242–d248.
3. Nikam A, Pagar T, Ghotekar S, Pagar K, Pansamble S. *Chem. Rev.*, 2019; **1(3):**154–163.
4. Iqbal J, Munir A, Uddin S. *Microsc. Res. Tech.*, 2020; **83**:706–719.
5. Rao TVM, Zahidi EM, Sayari A*J. Mol. Catal. A Chem.* 2009; **301**:159–165.
6. Patah A, Takasaki A, Szmyd JS. *Int.J. Hydrog. Energy,* 2009; **34**:3032–3037.
7. Rakesh S, Ananda S, Gowda NMM. *Mod. Res. Catal.* 2013; **2**:127–135.
8. 10. El-Sheikh SM, Mohamed RM, Fouad OA. *J. Alloys Compd.*, 2009; **482**:302–307.
9. Pei Z, Xu H, Zhang Y. *J Alloys Compd.,* 2009; **468**(1–2):5–8.
10. Sheng L, Feng-Li L, et al. *Chin Phys B.,* 2009; **18**:3985–3989.
11. El-Sheikh SM, Mohamed RM, Fouad OA. *J. Alloys Compd.*, 2009; **482**:302–307.
12. Fu XZ, Luo XX, Luo JL, Chuang KT, Sanger AR, Krzywicki A. *J Power Sources.,* 2001;**196(3):**1036–1041.
13. Ritu. *J. Appl. Chem.,* 2015; **8(3):**5–11.
14. Kim DW, Shin SI, Lee JD, Oh SG. *Mater Lett.,* 2004; **58**(12–13):1894–1898.
15. Farzaneh F, Naja M. *J. Sci. Islam Repub Iran,* 2011; **22(4)**:329–333.
16. Karimian R, Piri F, Davarpanah SJ. *J Appl Biotechnol Rep.,* 2014; **1(2):**73–76.
17. Rashed TR, Hamssa AE, Liblab SJ, AIP Conference Proceedings (2020); **2213**:020202-1 – 020202-7.
18. Henam Sylvia Devi, Muzaffar Ahmad Boda, Mohammad Ashraf Shah, Shazia Parveen, Abdul Hamid Wani.*Green Process Synth.,* 2019; **8**:38–45.
19. Chandran S, Rajesh P, Ramasamy P. Mater. Res. Bull., 2015; **68**:210–215.
20. Thangavelu S, Periyakali SB, Robin DS Joy. *Biological Trace Element Research,* 2018; 5.
21. Abdullah MM, Fahd M Raja, Saleh M Al-Abbas. *AIP ADVANCES,* 2014; **4**:027121-1 _207121-11.
22. Pawar NR,Chimankar OP, Bhandakkar VD, Padole NN, *J. Pure Appl. Ultrason*., 2012;**34**:49-52.